European Journal of Pharmacology 718 (2013) 261–270

Contents lists available at ScienceDirect

European Journal of Pharmacology

journal homepage: www.elsevier.com/locate/ejphar

Cardiovascular pharmacology

Local infiltration of neuropeptide Y as a potential therapeutic agent against apoptosis and fibrosis in a swine model of hypercholesterolemia and chronic myocardial ischemia

Robina Matyal [a,b,*], Sruthi Sakamuri [a], Angela Wang [a], Eitezaz Mahmood [a], Michael P. Robich [b,c], Kamal Khabbaz [b,c], Philip E. Hess [a,b], Frank W. Sellke [b,d,e], Feroze Mahmood [a,b]

[a] Beth Israel Deaconess Medical Center, Department of Anesthesia and Critical Care, CC-454, 1 Deaconess Road, Boston, MA 02215, USA
[b] Harvard Medical School, Boston, MA 02215, USA
[c] Beth Israel Deaconess Medical Center, Department of Surgery, USA
[d] Karlson and Karlson Professor of Cardiothoracic Surgery, Rhode Island Hospital, Cardiovascular Research Center, Department of Surgery, Providence, RI 02903, USA
[e] Alpert Medical School of Brown University, Providence, RI 02903, USA

ARTICLE INFO

Article history:
Received 15 May 2013
Received in revised form
23 July 2013
Accepted 26 August 2013
Available online 17 September 2013

Keywords:
Chronic ischemia
Oxidative stress
Fibrosis
Neuropeptide Y

ABSTRACT

While the angiogenic effects of Neuropeptide Y (NPY) in myocardial ischemia and hypercholesterolemia have been studied, its effects on altering oxidative stress, fibrosis and cell death are not known. We hypothesized that local infiltration of NPY in a swine model of chronic myocardial ischemia and hypercholesterolemia will induce nerve growth and cell survival, while reducing oxidative stress and fibrosis. Yorkshire mini-swine ($n=15$) were fed a high cholesterol diet for 5 weeks. Three weeks after surgical induction of focal myocardial ischemia, an osmotic pump was implanted, which delivered NPY ($n=8$, high cholesterol treated, HCT) or the vehicle ($n=7$, high cholesterol control, HCC) for 5 weeks. Then myocardium was harvested for analysis. Assessment of myocardial function and perfusion was made the last intervention. Immunoblotting demonstrated significantly decreased levels of MMP-9 ($p=0.001$) and TGF-β ($p=0.05$) and significantly increased levels of Ang-1 ($p=0.002$), MnSOD ($p=0.006$) and NGF ($p=0.01$) in HCT. Immunohistochemistry results revealed significantly decreased TUNEL staining ($p=0.005$) and GLUT4 translocation ($p=0.004$) in HCT. The functional data showed significantly improved blood flow reserve ($p=0.02$) and improved diastolic function $-dP/dt$ ($p=0.009$) in the treated animals. Local infiltration of NPY results in positive remodeling in ischemic myocardium in the setting of hypercholesterolemia. By initiating angio and neurogenesis, NPY infiltration improves blood flow reserve and restoration of fatty acid metabolism. The associated increased cell survival and decreased fibrosis result in improved myocardial diastolic function. NPY may have a potential therapeutic role in patients with hypercholesterolemia associated coronary artery disease.

1. Introduction

The etiology of coronary artery disease in patients with hypercholesterolemia and metabolic syndrome is multi-factorial (Boudina and Abel, 2010). Focused therapies with local infiltration of growth factors, gene and recombinant therapies have yielded mixed results, possibly due to the multi-faceted etiology of cardiac disease in metabolic syndrome (Khurana and Simons, 2003; Lassaletta et al., 2011). The altered angiogenic signaling and increased oxidative stress disrupts cellular metabolism resulting in increased cell death. Additionally, increased fibrosis associated with oxidative stress leads to pathological remodeling. The targeted biochemical therapy to attenuate mitochondrial dysfunction, cellular death, and fibrosis in the setting of hypercholesterolemia and metabolic syndrome has also been met with limited success (Calvani et al., 2000; Tocchetti et al., 2012). As a result, it is difficult to treat these patients with available percutaneous and conventional surgical revascularization procedures (Ali et al., 2012; Lassaletta et al., 2011; Levy et al., 1989). It has been suggested that Neuropeptide Y (NPY) a 36 amino acid neurotransmitter, may function as a "master switch" after full length NPY_{1-36} is cleaved to NPY_{3-36} in the myocardium (Khurana and Simons, 2003; Matyal et al., 2012). This cleavage stimulates trophic effects such as the

* Corresponding author at: Beth Israel Deaconess Medical Center, Department of Anesthesia and Critical Care, CC-454, 1 Deaconess Road, Boston, MA 02215, USA. Tel.: +1 617 754 2714; fax: +1 617 754 2677.
E-mail address: rmatyal@bidmc.harvard.edu (R. Matyal).

0014-2999/$ - see front matter © 2013 Elsevier B.V. All rights reserved.
http://dx.doi.org/10.1016/j.ejphar.2013.08.023

induction of hemodynamic, metabolic and growth-promoting properties at multiple levels (Matyal et al., 2012). The potential role of NPY in post-ischemic neo-vascularization has also been investigated in various studies (Hirsch and Zukowska, 2012; Lundberg et al., 1982; Matyal et al., 2012). Its ability to induce proliferation and hypertrophy of smooth muscle cells and cardiomyocytes has been reported in small animal studies for myocardial ischemia (Jacques et al., 2006a; Robich et al., 2010). Previous studies in swine models of myocardial ischemia have shown the local angiogenic effects of NPY on the myocardium including upregulation of pro-angiogenic markers, increased capillary and arteriolar formation, and decreased anti-angiogenic markers (Robich et al., 2010). Additionally, reduced myocardial levels of NPY have been implicated as a possible etiological factor for the observed autonomic neuropathy in diabetics (Levy et al., 1989; Matyal et al., 2011). While the trophic effects are well established, the effects of NPY on the prevention of cell death in the ischemic myocardium have not been studied (Baptista et al., 2012; Goncalves et al., 2012). It is quite possible that NPY acts at both ends of the cell cycle, inducing new cardiomyocyte growth and preventing cell death by altering oxidative stress and decreasing fibrosis.

Present in abundance in the intrinsic neurons of the myocardium and conduction system, NPY is released from the sympathetic nerve endings together with norepinephrine in response to acute and chronic stresses (Lassaletta et al., 2011). Specifically, NPY_{3-36} targets NPY Y2 receptors, which are involved more heavily in angiogenesis and capillary formation while uncleaved NPY_{1-36} and NPY_{31-34} also target NPY Y1 receptor, which affects vasoconstriction (Zukowska-Grojec et al., 1998). The ability of NPY to induce nerve growth in conjunction with angiogenesis and altering cardiomyocyte survival is not yet clearly established. Therefore, in this study we investigated the role of NPY_{3-36} in activating various cell survival pathways along with angio and neurogenesis to establish the impact of these changes in cell death, fibrosis and function. We hypothesized that local infiltration of NPY_{3-36} in the chronic ischemic myocardium in a swine model of hypercholesterolemia will induce nerve growth, prolong cell survival and alter fibrosis.

2. Methods

2.1. Animal model:

As previously described in a publication from our lab, all experiments were approved by hospital Institutional Animal Care and Use Committee. Animals were cared for in compliance with the Harvard Medical Area Institutional Animal Care and Use Committee and in accordance with the “Principles of Laboratory Animal Care” formulated by the National Society for Medical Research and the “Guide for the Care and Use of Laboratory Animals” (NIH Publication no. 5377-3, 1996).

Fifteen six-week-old male Yorkshire miniswine (Parsons Research, Amherst, MA) were used. After an initial period of 5 days for acclimatization the animals were fed 500 g of a hypercholesterolemic diet composed of 4% cholesterol, 17.2% coconut oil, 2.3% corn oil, 1.5% sodium cholate, and 75% regular chow daily. This hypercholesterolemia diet is known to induce metabolic syndrome in this swine model of hypercholesterolemia and chronic myocardial ischemia (Matyal et al., 2012). All animals had free access to water and were kept in a warm environment with minimal stress. The animals were fed for 5 weeks before the induction of myocardial ischemia and the diet was continued for the duration of the experiment.

2.2. Surgical protocol

After 5 weeks of dietary modification, all animals underwent the first surgical procedure. The day before each surgery, all animals received aspirin (325 mg orally) and were fasted for 12 h. Prior to each surgical procedure, all animals received prophylactic antibiotics and buprenorphine (0.03 mg/kg, intramuscular) for pain control. All survival procedures were conducted in a sterile fashion. For all surgical procedures, animals were given general anesthesia after sedating with Telazol (4 mg/kg, intramuscular), followed by endotracheal intubation and ventilation with a volume-cycled ventilator (North American Dragger). General anesthesia was maintained with a gas mixture of oxygen at 1.5–2 l/min and 3% isoflurane. The animal's vital signs were recorded during and throughout postoperative recovery. Femoral access via a percutaneously placed 4Fr sheath was achieved for arterial access, blood draws and blood pressure monitoring. An ameroid constrictor (internal diameter 1.75 mm) was placed on the proximal left circumflex coronary artery (LCx) via small left thoracotomy through the fourth intercostal space. During the first surgical procedure isotope-labeled microsphere (ILM) injection was performed to determine the myocardial territory at risk by temporary occlusion of the left circumflex artery and ILM injection in the left atrium.

Thirty minutes prior to the end of each procedure, a dose of buprenorphine (0.03 mg kg, intramuscular) was administered. After each procedure, the dosage of aspirin was continued for 5 days, while a fentanyl patch (4 ug/kg) was applied for 72 h for pain control. Animals demonstrating severe pain by refusing to eat, prostration, tachypnea tachycardia and listlessness were treated with an additional administration of fentanyl patch.

Three weeks after ameroid placement, the animals were anesthetized for the second time and coronary angiography was performed through femoral artery sheath to ensure occlusion of the LCx. Microsphere injection in the left atrium at rest and during ventricular pacing at a rate of 150 beats/min was performed through a mini-left thoracotomy. An osmotic pump (Alzet Inc. model 2ml4, Cupertino, CA, USA) was placed to deliver the peptide NPY_{3-36} solution (Sigma, Saint Louis, MO; NPY 60 μg mixed with 50 U of heparin in a 2 ml solution of 0.1% bovine serum albumin in phosphate buffered saline (PBS) delivered over 4 weeks at a rate of 3 μl/h) to eight animals on high cholesterol diet (HCT) (Matyal et al., 2012). Osmotic pump with placebo (0.1% bovine serum albumin in PBS) was placed in seven high cholesterol diet animals (HCC). The osmotic pump delivered drug directly into the ischemic territory via a catheter implanted into the myocardium at the first marginal branch of the LCx.

Five weeks after the osmotic pump placement, the animals were anesthetized for the third and final procedure. Coronary angiography was again performed through the femoral artery sheath, and the heart was exposed through median sternotomy and microspheres were injected at rest and with pacing in the left atrium. Lastly, sonomicrometer crystals (Sonometrics Corp. London, ON, Canada) were used to assess myocardial function. Following this, euthanasia was performed under deep anesthesia.

Myocardium was harvested and two 1 cm thick transversal slices cut at the mid-ventricular level and then sectioned into 8 segments identified clockwise starting from the anterior junction of the right and left ventricles. Separate samples were weighed and dried in a 60 °C oven for microsphere perfusion analysis. Samples from the anterior and lateral walls were taken for rapidly freezing in the liquid nitrogen for molecular studies or in 10% formaldehyde for paraffin section slides for immunohistochemistry.

The measurements for height and weight were made at the end of each procedure. Blood samples were collected after the femoral sheath placement and spun for serum and plasma analysis.

2.3. Myocardial perfusion analysis:

Myocardial perfusion was determined during each procedure with isotope-labeled microspheres (ILMs), which were 15 μm diameter (Biophysics Assay Laboratory) using previously reported methods (Robich et al., 2010). Briefly, 1.5×10^7 gold-labeled microspheres were injected during temporary LCx occlusion at the time of ameroid placement to identify the ischemic territory. The segments with the lowest concentration of gold ILMs were considered the area at risk. Labeled microspheres were also injected at the pump placement and final procedures during rest and ventricular pace (150 beats/min) conditions. Following euthanasia, 10 transmural left ventricular sections were collected for assays. The samples were exposed to neutron beams and microsphere densities were measured using a gamma counter.

2.4. Immunofluorescence labeling of GLUT4, PGP9.5 and beta-myosin

The immunofluorescence labeling of the paraffin embedded myocardial samples was performed with anti-Glut4 antibody. The paraffin sections were deparaffinized, rehydrated and treated with 10 mM Sodium Citrate pH 6.0 for antigen retrieval. The sections were then incubated with 1 mg/ml sodium borohdyride (ICN chemicals) for 5 min at room temperature. After three washes with TBS, the sections were incubated with 5% normal donkey serum (Jackson ImmunoResearch Lab Inc, West Grove, PA) for an hour at room temperature. Slides were then incubated with rabbit anti-Glut4 (1:100, Epitomics, Burlingame, CA), or mouse anti-PGP9.5 (1:100, Cedarlane) and Rabbit anti-MHY 7 (1:500, Sigma-Aldrich) overnight at 4 °C. The slides were washed three times and incubated with Dylight 649 conjugated Donkey anti-rabbit secondary antibodies (Jackson ImmunoResearch Lab, 1:200) and/or Dylight 549 Donkey anti- mouse secondary antibodies (Jackson ImmunoResearch Lab, 1:200) for 90 min at room temperature. Sections were then counterstained with Hoescht 33342 (Life Technologies, Woburn, MA) nuclear dye before they were mounted with Prolong Gold anti-fade mounting media (Life Technologies, Woburn, MA). Confocal images were taken using a Zeiss LSM510 Meta confocal system using Zeiss LSM510 image acquisition software. The images were taken using a 20 × /0.8 Plan-Apochromat objective and a 40 × /1.3 Oil Plan-Apochromat objective.

2.5. Sirius red collagen IHC staining on paraffin-embedding pig tissue

Sections were deparaffinized and hydrated. Nuclei were stained with Weigert's hematoxylin for 10 min and washed in water. Slides were stained with picro-sirius red (0.5 g Sirius red powder (F3B), 500 ml picric acid (saturated) solution) for 1 h and washed twice with acidified water (5 ml glacial acetic acid, 1 l distilled water). Water is removed through blotting with vigorous shaking. Slides are dehydrated three times in 100% ethanol, cleared in xylene, and mounted with permount. Images were analyzed using ImageJ.

2.6. IHC staining for TUNEL on paraffin-embedded pig tissue

Sections were deparaffinized in xylene, rehydrated through a downgraded series of alcohol solutions. The sections were then treated with Proteinase K (Sigma-Aldrich, St. Louis, MO) for 15 min at room temperature followed by incubation with 3% hydrogen peroxide at room temperature for 10 min. Endogenous biotin activity was quenched by Streptavidin/Biotin Blocking kit (Vector Laboratories, Burlingame, CA). The biotin-dUTP (Roche, Penzberg, Germany) labeling reaction mixture was added to the sections and incubated for 1 h at 37 °C. Thereafter, the sections were washed with Stop wash buffer (300 mM NaCl and 30 mM Sodium Citrate) for 10 min at room temperature. After rinsing the sections in TBS, the sections were incubated with HRP-streptavidin conjugates in TBS for 30 min at room temperature. Apoptotic nuclei were visualized by developing with DAB substrate kit (Vector Laboratories, Burlingame, CA). The slides were counterstained with hematoxylin, dehydrated through graded alcohols, cleared in xylene and mounted with Permount (Fisher).

2.7. Immunoblotting

Whole cell lysates were made from ischemic territory of the ischemic myocardium of both groups. Samples from both groups were run on the same gel to ensure identical conditions. Sixty micrograms of total protein was fractioned by a 4–12% gradient sodium dodecyl sulfate polyacrylamide gel electrophoresis (Life Technologies, Grand Island, NY) and transferred to PVDF membranes (Millipore, Billerica, MA) with a semi-dry transfer cell (Bio-Rad Trans-Blot, Hercules, CA). Ponceau staining was used to ensure equal protein loading. Each membrane was incubated with specific primary antibodies overnight at 4 °C and secondary antibodies for 1 h at room temperature. We examined fibrotic factors MMP-9 and TGF-β (Cell Signaling, Danvers, MA), anti-fibrotic factors p-Smad 1/5 (Cell Signaling, Danvers, MA), angiogenic factors Ang-1 (Santa Cruz Biotechnology, Santa Cruz, CA), mitochondrial metabolic factors PGC-1 and CPT1-M (Santa Cruz Biotechnology, Santa Cruz, CA), oxidative stress related factors MnSOD and HIF 1-alpha (R&D Systems, Minneapolis, MN & Cell Signaling Danvers, MA) and neurogenesis marker NGF (Santa Cruz Biotechnology, Santa Cruz, CA). Immune complexes were visualized with an enhanced chemiluminescence detection system (Amersham, Piscataway, NJ).

2.8. Data analysis:

All the results were expressed as mean ± standard deviation from the mean. Probability values of less than, or equal to, 0.05 were considered significant. The regional myocardial functional assessment by crystals was measured for left ventricular diastolic function ($-dP/dt$), vertical fractional shortening (VSS) for systolic function, and left ventricular cavity pressure. Immunoblots were analyzed after digitalization (ScabJet 4c; Hewlett Packard) with NIH ImageJ 1.33 software (National Institute of Health, Bethesda, MD). Comparison between the HCT group and the HCC group was analyzed by an unpaired, two-tailed *t*-test. The percentage of blood flow in the ischemic area after pacing was analyzed by the change in myocardial blood flow (ml/min/g tissue) derived from the myocardial microsphere concentration data, which was analyzed by Biophysics Assay Laboratories (Worcester, MA). The analysis was done using one-way ANOVA and Newman–Keuls multiple comparison post-hoc test. GraphPad Prism 4 (GraphPad Software, CA) was used for analysis.

3. Results

3.1. Experimental model

One pig in the HCT group died 1 week after the placement of osmotic pump. Autopsy identified congestive heart failure to be the cause of death. After the high cholesterol diet, the average body mass index (BMI) of the animals significantly increased ($p = 0.001$). Analysis of the plasma showed glucose intolerance and an elevation of apolipoprotein (apoB) reflecting an increase in all levels of proatherogenic particles after a high cholesterol diet (Table 1). Previously, we have shown that the associated changes in obesity, fasting glucose, and mean arterial pressure are suggestive of metabolic syndrome in high cholesterol diet swine (Grundy et al., 2004; Matyal et al., 2012).

3.2. Coronary angiography

The ameroid constrictor caused 100% occlusion of the LCx in all animals.

3.3. Left ventricular functional studies

There was significant improvement in diastolic function in HCT animals as compared to HCC animals (HCT 1802 ± 248 mmHg/s vs. HCC −1387 ± 247 mmHg/s, $p=0.009$). There was also increased vertical segmental shortening in the HCT group (HCT 16.1 ± 2.8 mm vs. HCC 13.2 ± 3.1 mm, $p=0.09$). There was no statistical change in the left ventricular pressure (HCT 80.4 ± 8.9mmHg vs. HCC 91.5 ± 26.0 mmHg, $p=0.3$) (Fig. 1).

3.4. Myocardial perfusion to the ischemic territory

The flow reserve (presented as percentage change) was measured as the ability to increase blood flow to the ischemic territory during cardiac pacing at 150 beats/min. It was significantly increased in HCT group as compared to the HCC group (142.2 ± 99.2% vs. 71.1 ± 47.5%, $p=0.02$) (Fig. 1).

3.5. Immunohistochemistry and immunoblotting

3.5.1. Angiogenesis

CD31 and smooth muscle actin staining of the myocardium show an increase in capillary density along with angiogenesis in the HCT tissue as compared with the HCC animals, as previously observed in this model (Robich et al., 2010). In HCT animals, immunoblotting showed significantly increased level of Ang-1, a pro-angiogenic protein that also plays an important role in the stabilization and maturation of new blood vessels ($p=0.002$) (Fig. 2).

Table 1
Baseline characteristics data: Comparison of mean body mass index (BMI) between the first surgery and the final surgery showed significant increase. Final blood sugar was calculated at the time of final surgery at fasting and 30 min after dextrose infusion suggested glucose intolerance. The comparison of apolipoprotein B (ApoB) levels between the first surgery and the final surgery showed no difference.

	Pre	Post	*p*-Value
BMI (kg/m ^ 2)	28.2 ± 2.5	40.1 ± 4.4	0.001
Blood glucose baseline (mg/dl)	53.9 ± 6.5	53.7 ± 15.0	0.60
Blood Glucose 30 min (mg/dl)	133 ± 33.6	129 ± 33.0	0.86
ApoB (g/ml)	1.30 ± 1.3	1.67 ± 2.1	0.46

3.5.2. Apoptosis of cardiomyocytes and fibrosis of myocardium

The number of TUNEL-positive cardiomyocytes in the ischemic tissue from HCT was significantly decreased as compared to that of the HCC group ($p=0.005$). Histological staining of the myocardium with picro-sirius red showed a marked decrease in collagen in the HCT group ($p=0.006$) as compared to the HCC animals. There was a significant decrease in the levels of pro-fibrotic and pro-apoptotic factors MMP-9 ($p=0.001$) and TGF-β group ($p=0.05$) in the HCT group, consistent with results for collagen staining and the TUNEL assay. The upstream anti-fibrotic and anti-apoptotic marker p-Smad 1/5 had an observed upward trend ($p=0.1$) in the HCT group, and is an inhibitor of TGF-beta signaling (Fig. 3).

3.5.3. Nerve expression, cardiomyocyte hypertrophy and proliferation

Ubiquitin carboxy-terminal hydrolase L1 (PGP9.5), a specific marker of neurons, makes up 1–2% of the soluble proteins in neurons. There was an observed increase in PGP9.5 expression in the HCT myocardium. Furthermore, beta-myosin correlated with areas of increased expression of PGP9.5. There was localized hypertrophy of cardiomyocytes in the perineural area of the HCT animals as described by beta-myosin expression. Immunoblotting of nerve growth factor was significantly increased in the myocardium of HCT pigs as compared to the control ($p=0.01$). There was no difference in proliferation measured by Ki-67 staining in both groups ($p=0.6$). (Fig. 4)

3.5.4. GLUT-4 receptor expression on the cardiomyocytes membranes and fatty acid metabolism:

GLUT4 expression was significantly decreased on the membranes of cardiomyocytes in the ischemic tissue of HCT pigs as compared to HCC group ($p=0.004$). Through immunoblotting assays, we observed a significant increase in the rate-limiting fatty acid oxidation factor CPT1-M in the HCT group ($p=0.005$). However, the levels of PGC-1, another factor involved in fatty acid oxidation, was significantly decreased in HCT group ($p=0.01$) (Fig.5).

3.5.5. Oxidative stress

The level of MnSOD, an important antioxidant with cardioprotective effects, was significantly increased in the HCT group ($p=0.006$). The level of HIF1-α, a factor upregulated during oxidative stress, was significantly decreased in HCT pig tissue as compared to HCC ($p=0.004$). The significant decrease in HIF1-α in HCT suggests a decrease in reactive oxygen species thus decreased oxidative stress (Fig. 6).

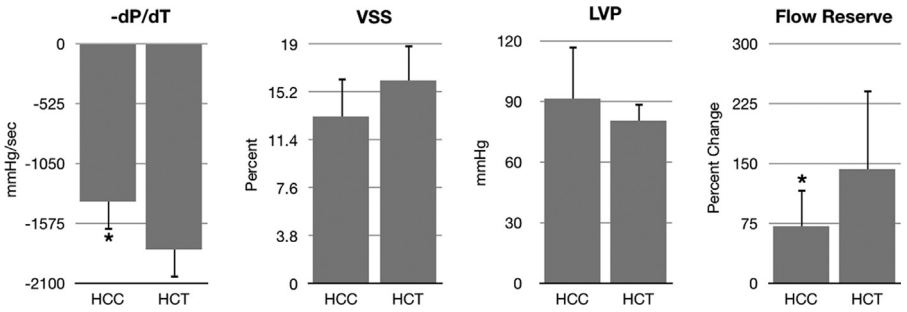

Fig. 1. Myocardial function and perfusion: Invasively driven left ventricular functional data comparing diastolic function ($-dP/dt$), systolic function as measured by vertical segment shortening (VSS) and left ventricular pressure (LVP) There was significant improvement in $-dP/dt$ in the HCT group). There was no significant difference in VSS and LVP between the groups. The increase in flow reserve, the ability to increase blood flow in the ischemic territory when paced at 150 beats/min presented as percentage change was measured by microsphere injection. There was significant increase in flow reserve in the HCT group.

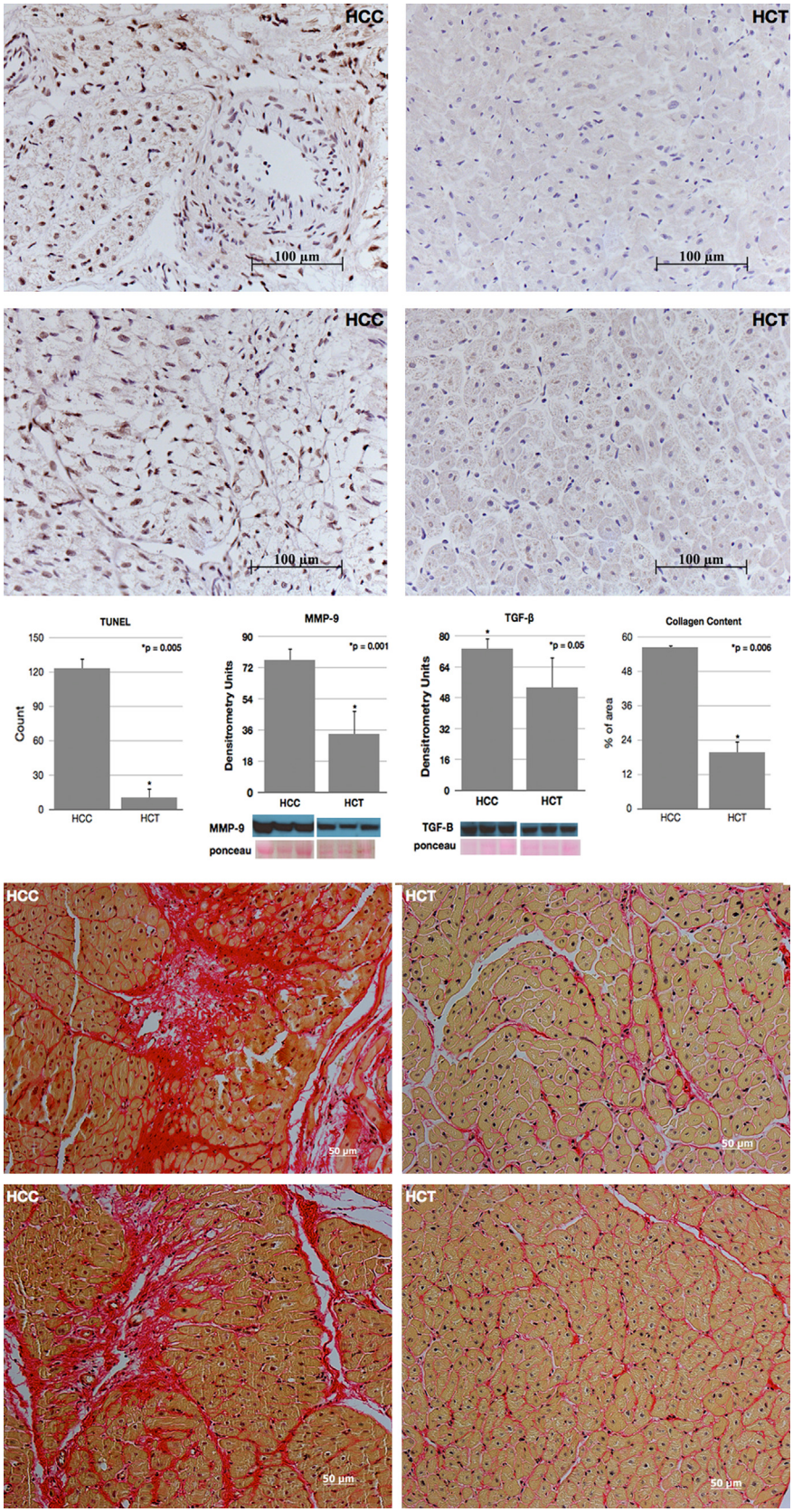

Fig. 2. Apoptosis and fibrosis: There is significantly decreased TUNEL staining in cardiomyocytes in the HCT as compared to HCC group. Sirius red staining of myocardium shows a significant decrease in myocardial fibrosis in the HCT group. Expression of pro-fibrotic/pro-apoptotic, anti-fibrotic and pro-angiogenic proteins was measured by immunoblotting. There was significant decrease in pro-fibrotic proteins TGF-β and MMP-9 levels in HCT group. The levels of anti-fibrotic protein p-Smad 1/5 were increased in HCT group.

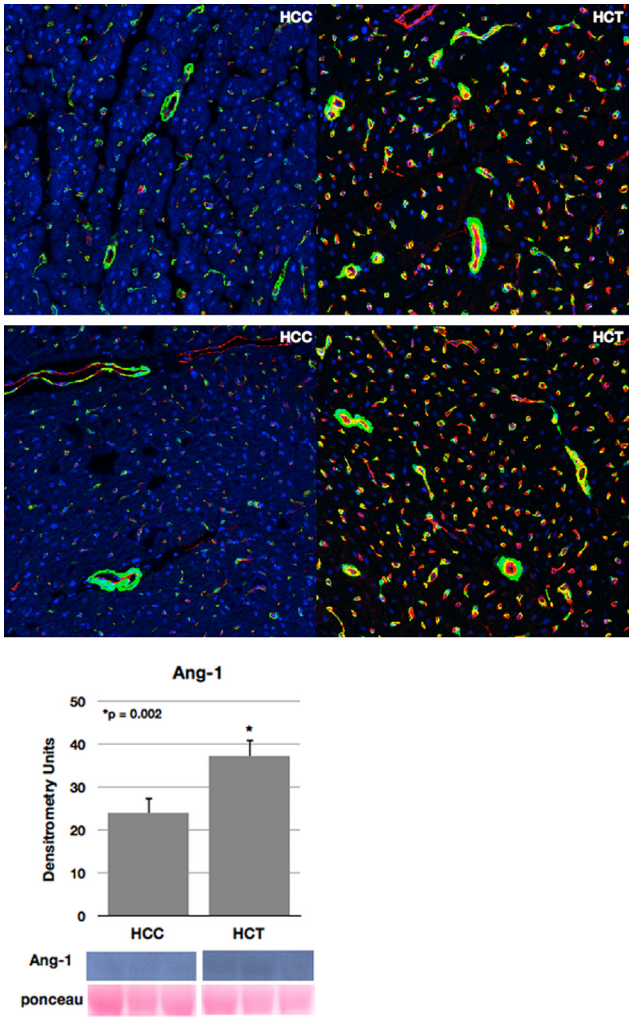

Fig. 3. Angiogenesis: Capillary density is also increased in the HCT group as seen in the stained myocardium with CD31 in red, SMA (smooth muscle actin) in green, and DAPI for nuclei staining. Angiogenesis: The levels of Ang-1 a potent angiogenic marker was increased in HCT group. (For interpretation of the references to color in this figure legend, the reader is referred to the web version of this article.)

4. Discussion

We have demonstrated the multifaceted effects of NPY_{3-36} in reversing the maladaptive remodeling at molecular, histological and functional levels. Observed increases within the treated animals in nerve growth as well as a possible angiogenesis-related increase of antioxidants and decrease in hypoxia signaling occurred despite the hypercholesterolemic milieu. Simultaneously, we observed a significant decrease in pro-fibrotic signaling and thus, fibrosis. The aforementioned effects were associated with a significant decrease in cell death. At the functional level, NPY regulation of neuro and angiogenesis resulted in increased blood flow reserve in the ischemic myocardial territory. Favorable effects were also observed physiologically as an improvement in left ventricular relaxation and systolic fractional shortening. As a result, we conclude that not only does local infiltration have trophic effects but also suggests increased cell survival by inhibition of apoptosis (Fig. 7).

Although NPY has been known to have a widespread vasoconstrictor effect which could improve perfusion and ventricular function, we have seen local histological effects of NPY_{3-36}, which corroborate with the findings in the functional data to produce these beneficial effects due to the specificity of the cleaved product. The dosage required to observe angiogenic effects of NPY is much lower than that required to cause vasoconstriction and hypertension (Zukowska-Grojec et al., 1998). Along with sub-therapeutic dosage determined from previous swine studies, cleaved product NPY_{3-36} also specifically targets the angiogenic function rather than vasoconstrictor function of NPY (Robich et al., 2010; Matyal et al., 2012). Previous studies also show that the physiological dose of NPY administered via pump did not exhibit overall systemic effects witnessed in animals with larger doses of systemically-administered NPY (Matyal et al., 2012; Zukowska-Grojec et al., 1998).

Metabolic syndrome and hypercholesterolemia are associated with endothelial dysfunction and maladaptive stress response. During metabolic syndrome, there is an increased expression of anti-angiogenic factors (angiostatin and endostatin), which has been documented in both animal and human studies (Jacques et al., 2006a; Jacques et al., 2006b; Jacques et al., 2003; Matyal et al., 2011). Additionally, ischemia is known to increase oxidative stress and cell death, through elevated MMP-9 and TGF-β levels, causing fibrosis and apoptosis in this patient population (Ali et al., 2012; Boudina and Abel, 2010; Ovechkin et al., 2005) Targeted therapies could lack efficacy partly due to multifaceted physical derangements in this complex disease process. The NPY-related histological reduction in fibrosis at the cellular level coupled with improved physiological relaxation suggests a cause and effect relationship. Furthermore, our demonstration of the ability of NPY to activate transcription cascades for angiogenesis and neurogenesis as well as enhance antioxidant environment and improve cell survival provides critical information that may lead to treatment of this disease.

The multifaceted role of NPY (neurohormone, growth factor, neurotransmitter and an inflammatory mediator) has been shown to extend across species (Hirsch and Zukowska, 2012; Robich et al., 2010). The levels of NPY secreting sympathetic nerve endings are higher during the postnatal ontogenesis time period and gradually decrease over time (Nozdrachev and Masliukov, 2011). Its specific localization and abundance in the heart has an important role in chronic stress response (Jacques et al., 2006a, 2003) Furthermore, the levels of NPY Y2 receptor are known to decrease in old age, secondary to a decreased ability for angiogenesis (Morrison et al., 2009). The downregulated levels of NPY in diabetic myocardium could be responsible for the autonomic dysfunction and impaired trophic activity (Chottova Dvorakova et al., 2008; Levy et al., 1989; Nozdrachev and Masliukov, 2011).

Elevated levels of NGF show a marked improvement in the myocardium as the factor is usually downregulated in diabetes mellitus [9]. Also, NGF gene therapy has previously been shown to improve sensory innervation and neuropathy in diabetic mice hearts (Hellweg and Hartung, 1990; Ieda et al., 2006). The ability of exogenously delivered NPY to stimulate neurogenesis in our swine model of hypercholesterolemia, chronic ischemia, and metabolic syndrome might also have therapeutic implications.

The potential role of NPY signaling in energy homeostasis regulation has been reported in peripheral tissue. Appending previous research, we observed a possible new mitochondrial membrane stabilizing effect of NPY. An increase in mitochondrial membrane residing MnSOD within treated animals shows a potential benefit of NPY as upregulated levels of MnSOD have been shown to be cardioprotective against oxidative stress in hyperglycemic conditions (Ivanovic-Matic et al., 2010; Kim et al., 2008). The NPY-treated myocardium also demonstrated an increase in the CPT1-M activity, a rate-limiting step in fatty acid metabolism in the mitochondrial membrane. Previous studies have shown that CPT1-M is decreased in animals with depleted levels of NPY Y2 receptors, leading to imbalances of the lipolytic and lipogenic pathways (Sanchez-Lasheras et al., 2010). The up-regulation of

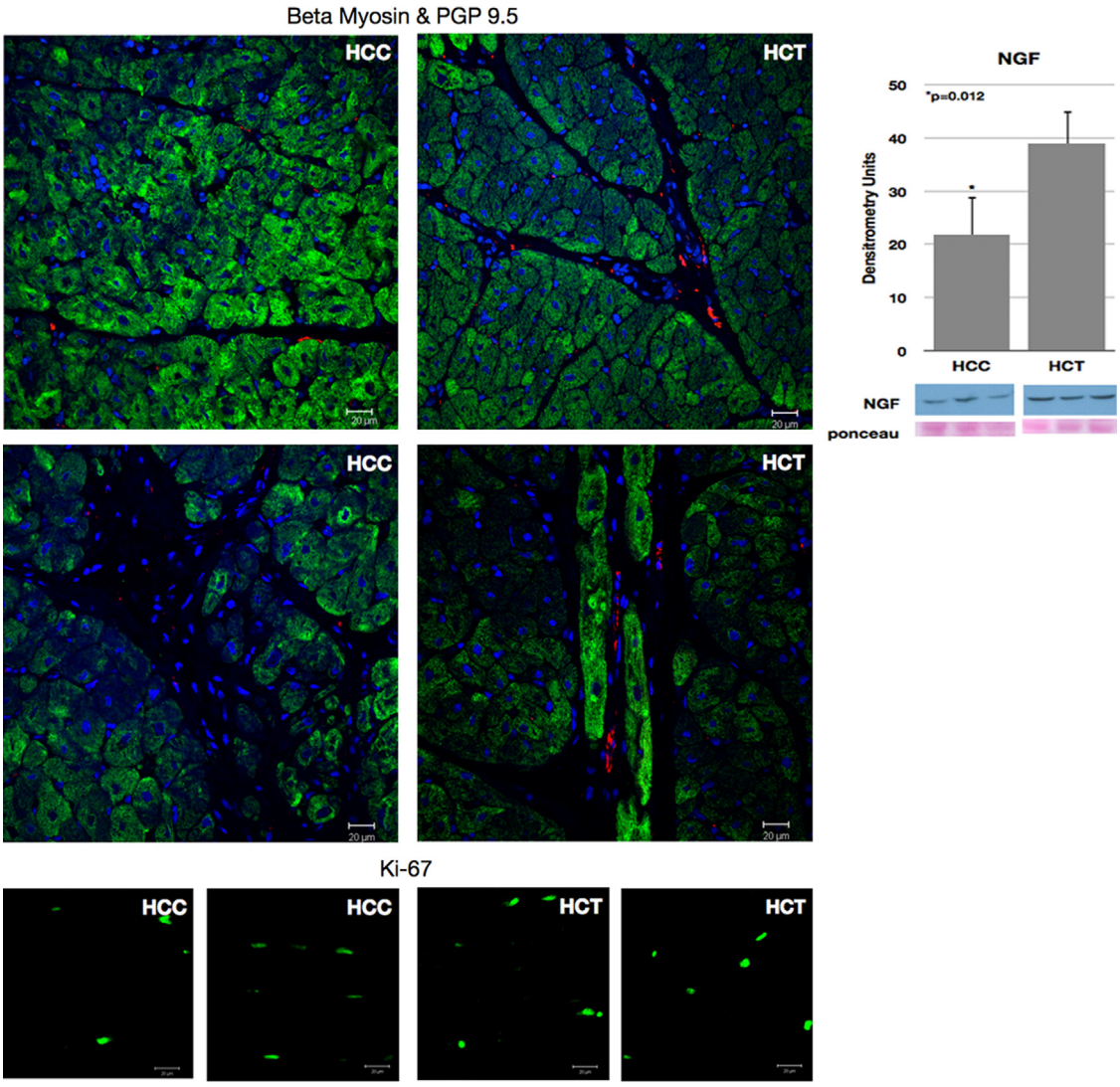

Fig. 4. Hypertrophy/nerve growth/proliferation: The slides were co-stained with sympathetic nerve specific PGP9.5 (red) and cardiomyocyte hypertrophy marker Beta-myosin (green) and stained for nuclear proliferation marker Ki-67 (green). There was markedly increased nerve expression in the HCT group. There was an increase in hypertrophic cardiac cells within the perineural area. Additionally, there was no statistical difference in proliferation between the HCC and HCT group. All scale bars represent 20 μm. Using immunoblotting, a significant upregulation of nerve growth factor (NGF) is observed in the HCT group. (For interpretation of the references to color in this figure legend, the reader is referred to the web version of this article.)

CPT1-M along with reduced expression of GLUT-4 receptors in cardiomyocytes is further evidence of decreased oxidative stress and the restoration of cardiac mitochondrial fatty acid metabolism. The decreased fibrosis and improved diastolic function of the myocardium after NPY-treated transplantation of mesenchymal cells have been previously observed in a rat acute model of myocardial ischemia (Wang et al., 2010). While an exact cause and effect relationship are difficult to establish, the restoration of blood flow to the ischemic area could be responsible for the physiological improvement. The upregulation of Ang-1 to develop mature and non-leaky vessels leads to increased blood flow reserve in the treated ischemic area and improves myocardial function while also inhibiting myocardial apoptosis (Chen and Stinnett, 2008; Zeng et al., 2012).

4.1. Limitations

Even though we were able to show changes at molecular and cellular levels in the swine model of metabolic syndrome and chronic myocardial ischemia, the time frame for the development of metabolic syndrome and the time frame of myocardial ischemia are short and may not be an actual representation of the chronic disease in humans. Similarly, the exposure to treatment with NPY was abbreviated as well. It remains to be seen whether the benefit is temporary or if treatment for a longer time is beneficial. Also, we were not able to see marked difference in proliferation of cardiomyocytes another reported effect of NPY, possibly due to limited time frame for treatment. Further testing of the restoration of mitochondrial function after ischemia and hypercholesterolemia would be able to elucidate the full extent of effects of NPY.

5. Conclusion

The local infiltration of NPY_{3-36} in ischemic myocardium can up-regulate key cell survival pathways to counter chronic hypoxic stress leading to effective remodeling. By acting as a multifaceted trophic and homeostasis regulator, NPY initiated angiogenesis leads to improved vascular reserve and less oxidative stress on the mitochondria thus shifting cellular metabolism back to fatty acid oxidation and increasing markers of cell survival. The NPY_{3-36}-related remodeling led to neurogenesis and angiogenesis

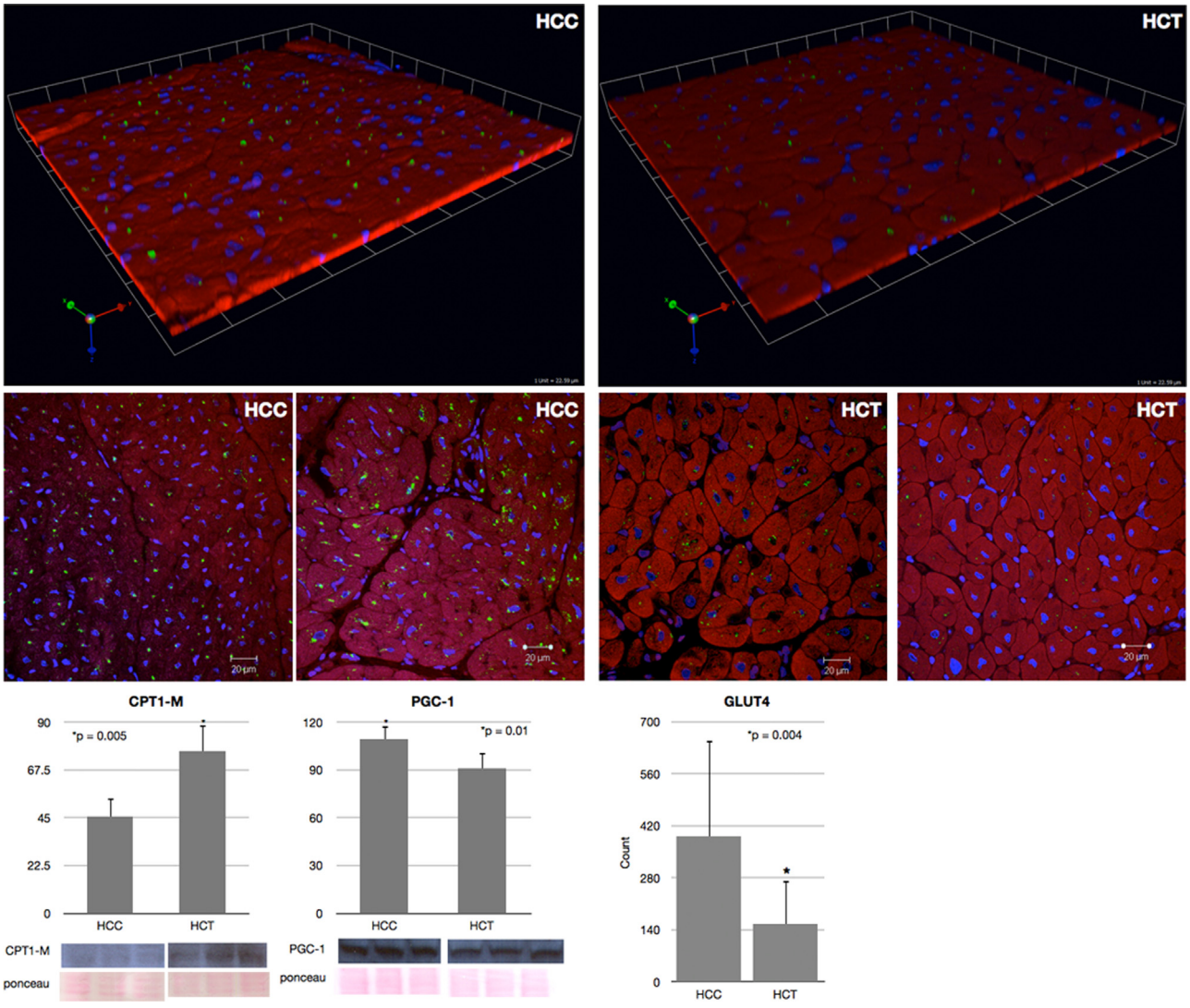

Fig. 5. Glucose and fatty acid metabolism: The slides were co-stained with specific glucose receptors GLUT-4 (green), cardiomyocytes (red) and nuclei (DAPI, blue). There was significant decrease in GLUT4 transporters in the membrane of cardiomyocytes in the HCT group as opposed to HCC group. Each unit in the grid represents 22.5 μm. CPT1-M a rate limiting protein for long chain fatty acid metabolism was significantly increased in HCT group, while PGC-1 another protein for fatty acid metabolism was decreased in HCT group. (For interpretation of the references to color in this figure legend, the reader is referred to the web version of this article.)

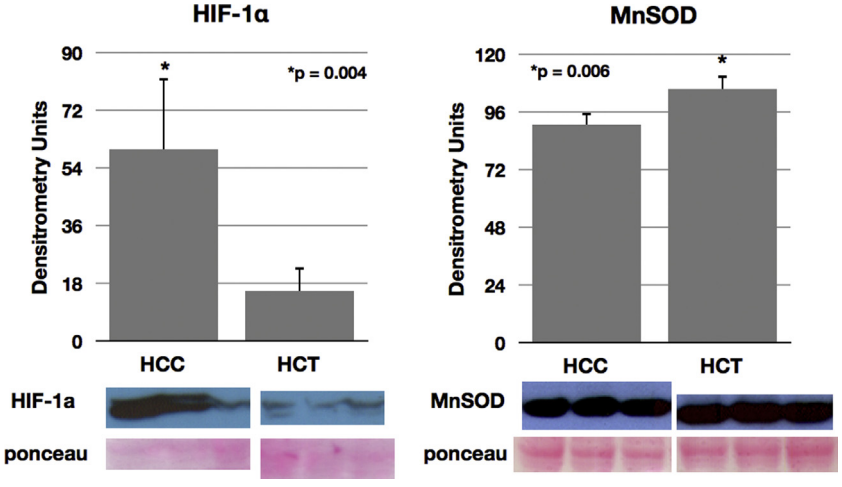

Fig. 6. Oxidative stress: Expression of antioxidant, oxidative stress and fatty acid metabolism proteins was measured by immunoblotting. There was significant increase in anti-oxidant protein MnSOD and decrease in hypoxia induced protein HIF-1α.

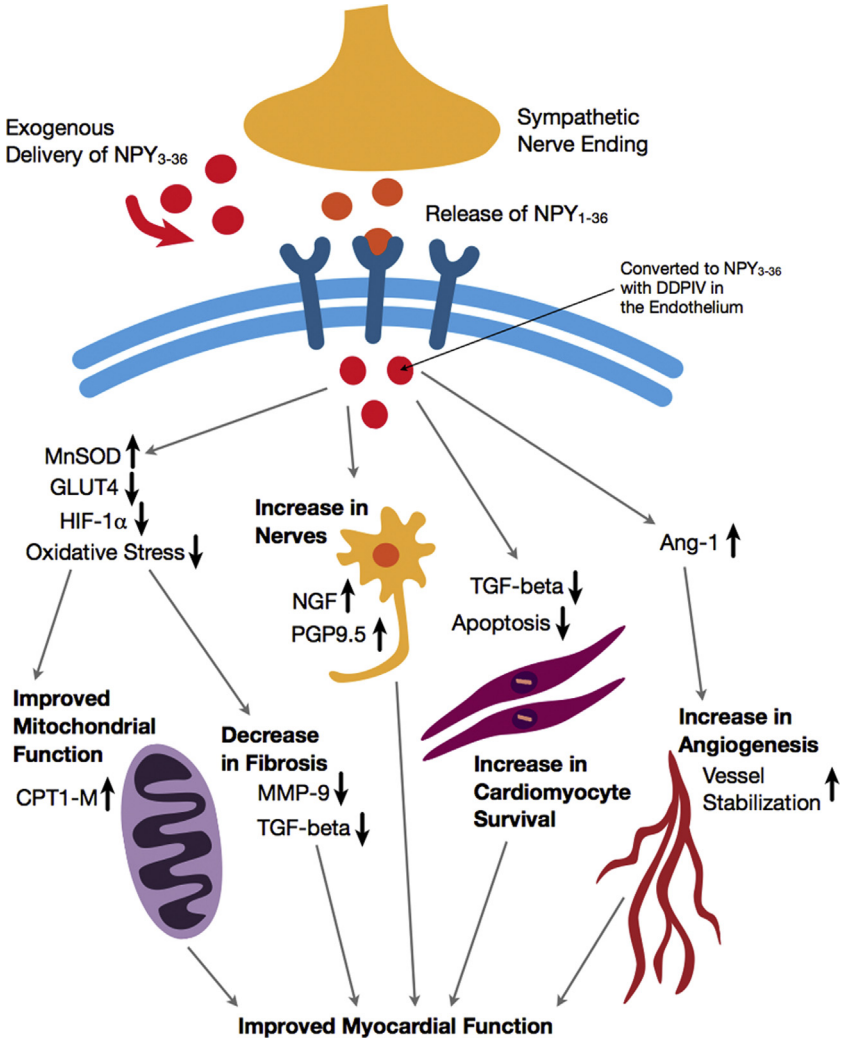

Fig. 7. Overview: Summary of the proposed mechanism for observed increase in nerve expression, cell survival and reduced fibrosis influenced by exogenous NPY_{3-36}. Exogenously delivered NPY_{3-36} causes angiogenesis and nerve growth via the upregulation of several factors. It causes increase in anti-oxidant and fatty acid metabolic enzymes, stabilizing the mitochondrial membrane and improving energy homeostasis. There is resultant increase in cardiomyocytes survival and decreased fibrosis. Positive remodeling of cardiac tissue along with increased angio/neurogenesis leads to improved blood flow and myocardial function especially diastolic function in the ischemic myocardium in the swine model of metabolic syndrome and hypercholesterolemia. Image created with Adobe Illustrator.

possibly causing increased cell survival and decreased fibrosis thus improving diastolic function. NPY_{3-36} has a potential therapeutic role in patients with metabolic syndrome and hypercholesterolemia associated coronary artery disease and cardiomyopathy.

6. Disclosures

None.

References

Ali, S., Shakil, O., Chen, T.H., Warraich, H.J., Matyal, R., 2012. An incidental finding during emergent vascular surgery: how far to go? Journal of Cardiothoracic and Vascular Anesthesia 26, 354–355.

Baptista, S., Bento, A.R., Goncalves, J., Bernardino, L., Summavielle, T., Lobo, A., Fontes-Ribeiro, C., Malva, J.O., Agasse, F., Silva, A.P., 2012. Neuropeptide Y promotes neurogenesis and protection against methamphetamine-induced toxicity in mouse dentate gyrus-derived neurosphere cultures. Neuropharmacology 62, 2413–2423.

Boudina, S., Abel, E.D., 2010. Diabetic cardiomyopathy, causes and effects. Reviews in Endocrine and Metabolic Disorders 11, 31–39.

Calvani, M., Reda, E., Arrigoni-Martelli, E., 2000. Regulation by carnitine of myocardial fatty acid and carbohydrate metabolism under normal and pathological conditions. Basic Research in Cardiology 95, 75–83.

Chen, J.X., Stinnett, A., 2008. Ang-1 gene therapy inhibits hypoxia-inducible factor-1alpha (HIF-1alpha)-prolyl-4-hydroxylase-2, stabilizes HIF-1alpha expression, and normalizes immature vasculature in db/db mice. Diabetes 57, 3335–3343.

Chottova Dvorakova, M., Wiegand, S., Pesta, M., Slavikova, J., Grau, V., Reischig, J., Kuncova, J., Kummer, W., 2008. Expression of neuropeptide Y and its receptors Y1 and Y2 in the rat heart and its supplying autonomic and spinal sensory ganglia in experimentally induced diabetes. Neuroscience 151, 1016–1028.

Goncalves, J., Ribeiro, C.F., Malva, J.O., Silva, A.P., 2012. Protective role of neuropeptide Y Y(2) receptors in cell death and microglial response following methamphetamine injury. European Journal of Neuroscience 36, 3173–3183.

Grundy, S.M., Brewer Jr., H.B., Cleeman, J.I., Smith Jr., S.C., Lenfant, C., 2004. Definition of metabolic syndrome: report of the national heart, lung, and blood institute/American Heart Association conference on scientific issues related to definition. Circulation 109, 433–438.

Hellweg, R., Hartung, H.D., 1990. Endogenous levels of nerve growth factor (NGF) are altered in experimental diabetes mellitus: a possible role for NGF in the pathogenesis of diabetic neuropathy. Journal of Neuroscience Research 26, 258–267.

Hirsch, D., Zukowska, Z., 2012. NPY and stress 30 years later: the peripheral view. Cellular and Molecular Neurobiology 32, 645–659.

Ieda, M., Kanazawa, H., Ieda, Y., Kimura, K., Matsumura, K., Tomita, Y., Yagi, T., Onizuka, T., Shimoji, K., Ogawa, S., Makino, S., Sano, M., Fukuda, K., 2006. Nerve growth factor is critical for cardiac sensory innervation and rescues neuropathy in diabetic hearts. Circulation 114, 2351–2363.

Ivanovic-Matic, S., Mihailovic, M., Dinic, S., Martinovic, V., Bogojevic, D., Grigorov, I., Poznanovic, G., 2010. The absence of cardiomyopathy is accompanied by increased activities of CAT, MnSOD and GST in long-term diabetes in rats. Journal of Physiological Sciences 60, 259–266.

Jacques, D., Sader, S., Perreault, C., Abdel-Samad, D., 2006a. NPY and NPY receptors: presence, distribution and roles in the regulation of the endocardial endothelium and cardiac function. EXS, 77–87.

Jacques, D., Sader, S., Perreault, C., Abdel-Samad, D., Provost, C., 2006b. Roles of nuclear NPY and NPY receptors in the regulation of the endocardial endothelium and heart function. Canadian Journal of Physiology and Pharmacology 84, 695–705.

Jacques, D., Sader, S., Perreault, C., Fournier, A., Pelletier, G., Beck-Sickinger, A.G., Descorbeth, M., 2003. Presence of neuropeptide Y and the Y1 receptor in the plasma membrane and nuclear envelope of human endocardial endothelial cells: modulation of intracellular calcium. Canadian Journal of Physiology and Pharmacology 81, 288–300.

Khurana, R., Simons, M., 2003. Endothelial progenitor cells: precursors for angiogenesis. Seminars in Thoracic and Cardiovascular Surgery 15, 250–258.

Kim, J.A., Wei, Y., Sowers, J.R., 2008. Role of mitochondrial dysfunction in insulin resistance. Circulation Research 102, 401–414.

Lassaletta, A.D., Chu, L.M., Sellke, F.W., 2011. Therapeutic neovascularization for coronary disease: current state and future prospects. Basic Research in Cardiology 106, 897–909.

Levy, D.M., Karanth, S.S., Springall, D.R., Polak, J.M., 1989. Depletion of cutaneous nerves and neuropeptides in diabetes mellitus: an immunocytochemical study. Diabetologia 32, 427–433.

Lundberg, J.M., Terenius, L., Hokfelt, T., Martling, C.R., Tatemoto, K., Mutt, V., Polak, J., Bloom, S., Goldstein, M., 1982. Neuropeptide Y (NPY)-like immunoreactivity in peripheral noradrenergic neurons and effects of NPY on sympathetic function. Acta Physiologica Scandinavica 116, 477–480.

Matyal, R., Chu, L., Mahmood, F., Robich, M.P., Wang, A., Hess, P.E., Shahul, S., Pinto, D.S., Khabbaz, K., Sellke, F.W., 2012. Neuropeptide Y improves myocardial perfusion and function in a swine model of hypercholesterolemia and chronic myocardial ischemia. Journal of Molecular and Cellular Cardiology 53, 891–898.

Matyal, R., Mahmood, F., Robich, M., Glazer, H., Khabbaz, K., Hess, P., Bianchi, C., Hagberg, R., Hu, S.X., Sellke, F.W., 2011. Chronic type II diabetes mellitus leads to changes in neuropeptide Y receptor expression and distribution in human myocardial tissue. European Journal of Pharmacology 665, 19–28.

Morrison, J.F., Dhanasekaran, S., Howarth, F.C., 2009. Neuropeptide Y and CGRP concentrations in the rat tail artery: effects of age and two types of diabetes. Peptides 30, 710–714.

Nozdrachev, A.D., Masliukov, P.M., 2011. Neuropeptide Y and autonomic nervous system. Zhurnal Evoliutsionnoĭ Biokhimii i Fiziologii 47, 105–112.

Ovechkin, A.V., Tyagi, N., Rodriguez, W.E., Hayden, M.R., Moshal, K.S., Tyagi, S.C., 2005. Role of matrix metalloproteinase-9 in endothelial apoptosis in chronic heart failure in mice. Journal of Applied Physiology 99, 2398–2405.

Robich, M.P., Matyal, R., Chu, L.M., Feng, J., Xu, S.H., Laham, R.J., Hess, P.E., Bianchi, C., Sellke, F.W., 2010. Effects of neuropeptide Y on collateral development in a swine model of chronic myocardial ischemia. Journal of Molecular and Cellular Cardiology 49, 1022–1030.

Sanchez-Lasheras, C., Konner, A.C., Bruning, J.C., 2010. Integrative neurobiology of energy homeostasis-neurocircuits, signals and mediators. Frontiers in Neuroendocrinology 31, 4–15.

Tocchetti, C.G., Caceres, V., Stanley, B.A., Xie, C., Shi, S., Watson, W.H., O'Rourke, B., Spadari-Bratfisch, R.C., Cortassa, S., Akar, F.G., Paolocci, N., Aon, M.A., 2012. GSH or palmitate preserves mitochondrial energetic/redox balance, preventing mechanical dysfunction in metabolically challenged myocytes/hearts from type 2 diabetic mice. Diabetes 61, 3094–3105.

Wang, Y., Zhang, D., Ashraf, M., Zhao, T., Huang, W., Ashraf, A., Balasubramaniam, A., 2010. Combining neuropeptide Y and mesenchymal stem cells reverses remodeling after myocardial infarction. American Journal of Physiology: Heart and Circulatory Physiology 298, H275–H286.

Zeng, H., Li, L., Chen, J.X., 2012. Overexpression of angiopoietin-1 increases $CD133^{+}$/c-$kit^{\pm}$ cells and reduces myocardial apoptosis in db/db mouse infarcted hearts. PLOS ONE 7, e35905.

Zukowska-Grojec, Z., Karwatowska-Prokopczuk, E., Rose, W., Rone, J., Movafagh, S., Ji, H., Yeh, Y., Chen, W.T., Kleinman, H.K., Grouzmann, E., Grant, D.S., 1998. Neuropeptide Y: a novel angiogenic factor from the sympathetic nerves and endothelium. Circulation Research 83 (2), 187–195.